DISCRETE AND CONTINUOUS
DYNAMICAL SYSTEMS
Supplement 2009

Website: www.aimSciences.org

pp. **753–760**

A SIMPLE MODEL OF TWO INTERACTING SIGNALING PATHWAYS IN EMBRYONIC *XENOPUS LAEVIS*

Edwin Tecarro

Department of Computer and Mathematical Sciences
University of Houston-Downtown, Houston, Texas 77002-1001, USA

Tung Bui

Department of Natural Sciences
University of Houston-Downtown, Houston, Texas 77002-1001, USA

Marsida Lisi

Department of Computer and Mathematical Sciences
University of Houston-Downtown, Houston, Texas 77002-1001, USA

Amy Sater

Department of Biology and Biochemistry
University of Houston, Houston, Texas 77204-5001 , USA

Akif Uzman

Department of Natural Sciences
University of Houston-Downtown, Houston, Texas 77002-1001, USA

Abstract. A mathematical model of MAPK and BMP-Smad1 signaling pathways in the embryonic development of *Xenopus laevis* is constructed. The model consists of a system of 4 coupled, nonlinear ordinary differential equations. Numerical computations characterize the biological result that a 4 to 6-fold increase in MAPK activity inhibits Smad1 activity and triggers the neural fate of the embryo's ectodermal cells. Bifurcation analysis of the model shows that this biological result can be explained via transcritical bifurcations involving steady-state MAPK and Smad1 activity levels.

1. **Introduction.** The development of vertebrate embryos is heavily dependent on intercellular communication mediated by families of extracellular signals, originally identified as Peptide Growth Factors (PGFs). Two of these families, Fibroblast Growth Factors (FGFs) and Bone Morphogenetic Proteins (BMPs) act together to regulate a wide range of processes during vertebrate embryonic development. In most instances, these signals act to promote opposing developmental pathways, and the final outcome reflects the local balance between the two. For example, FGFs promote limb bud outgrowth, while BMPs cause limb bud cells to withdraw from the cell cycle [1]. During mammalian tooth development, high FGF signaling is required to initiate tooth formation, and tooth formation is inhibited by BMPs [2]. Proepicardial cells, which contribute to both cardiomyocytes and the epicardial lining, select between these fates based on exposure to either FGFs, which

2000 *Mathematics Subject Classification.* Primary: 92B99; Secondary: 37N25.

Key words and phrases. mathematical model, signaling pathway, transcritical bifurcation, MAPK, BMP.

induce epicardial differentiation, or BMPs which induce cardiomyocyte differentiation [3]. In amphibian embryos, BMPs induce blood formation, while FGFs inhibit the specification of blood progenitors [4]. In the interdigital region of the limb bud, BMPs trigger programmed cell death (apoptosis), whereas FGFs protect cells from programmed cell death [5].

BMPs and FGFs also regulate specification of vertebrate ectoderm. BMPs induce epidermal differentiation, while FGFs (with contributions from Insulin-like Growth factor, or IGF, which activates the same intracellular pathways) elicit specification of neural ectoderm; inhibition of BMP signaling is also required for the establishment of neural fate (reviewed in [6]; [7]). The critical intracellular pathway activated by FGF is the erk MAPK pathway (MAPK); MAPK activity is necessary for the initiation of neural development. Earlier studies have demonstrated that the effector pathways activated by FGF and BMP4 interact via mutually antagonistic crosstalk ([8], [9], [10], [11]). Moreover, MAPK activity increases 4 to 6-fold within the future neural ectoderm during the period of neural specification *in vivo*, and disruption of BMP signaling is sufficient to generate an increase in MAPK [12].

2. **Model Development.** A mathematical model is constructed with the aim of further understanding the interaction between the BMP-Smad1 pathway (which leads to the expression of epidermal genes) and the MAPK pathway activated by fibroblast growth factor (FGF) (which leads to the expression of neural genes) in the embryonic development of the frog *Xenopus laevis*. These pathways are diagrammed in Figure 1.

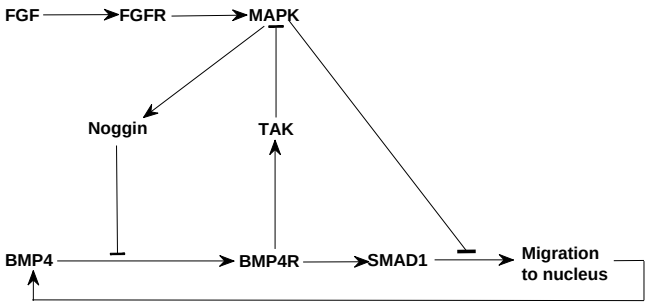

FIGURE 1. Diagram of two interacting signaling pathways.

The development of mathematical models that describe each of these signaling pathways is a current area of active research. Huang and Ferrell [13] described the MAPK cascade, which is a highly conserved series of protein kinases implicated in diverse biological processes. Their model consists of a 18 coupled, nonlinear ordinary differential equations and exhibits bistable and periodic solutions [14]. Muller, *et al.* [15] modeled the FGF-MAPK network with a system consisting of 106 ordinary differential equations. They further studied a reduced 6-node version of this network that encompasses the rate-limiting process; it sustains the feedback loops and provides sufficient information to predict biological responses. To study the mesodermal induction in *Xenopus* embryos, Diaz, *et al.* [16] developed a model which describes the interaction of the MAPK pathway with the $IP_3 - Ca^{2+}$ pathway. In this particular model, they justified the use of a single variable to describe a

significant portion of the MAPK pathway. Clarke and Liu [17] reviewed the mathematical models of the TGF-β superfamily of ligands (of which BMP is a member). They described the motivation for modeling studies of TGF-β signaling and discuss how first-generation models have contributed to the understanding of TGF-β biology. Among these models, they cited the work of Schmierer, *et al.* [18] on a 15-variable system of ordinary differential equations that describe the BMP-Smad network.

Although there are numerous proteins involved in the MAPK and BMP-Smad1 signaling pathways, some assumptions make the development of a simple mathematical model possible. The model discussed in this paper focuses on the activity of four protein or protein groups that have been observed to be significant players in the interaction of these pathways. With regard to the MAPK pathway, we assume that FGF binds immediately to its receptor FGFR and the bound FGF automatically activates MAPK and activated MAPK leads indirectly to Noggin production. This assumption enables us to represent the entire MAPK pathway by a single variable, M. For the BMP-Smad1 pathway, we assume that BMP immediately binds to its receptor BMP4R, and that as soon as Smad1 is activated by the bound BMP, it immediately forms a complex with SMAD4. In the model, this pathway is represented by two variables: B, for the activity of the bound BMP, and S, for the activity of the Smad1/4 complex, which is entirely dependent upon the level of activated Smad1. We include the activity of TAK1 (represented by T) in the model, since it is an intermediary protein that significantly affects both MAPK and Smad1/4 activity. TAK1 is assumed to have a negative regulatory effect on Smad1: this is based on experimental findings that show that TAK1 binds to Smad1 and inhibits Smad1 nuclear translocation ([19], [20]).

Based on the diagram in Figure 1, we develop the following system of nonlinear and coupled ordinary differential equations to describe the interaction of the two signaling pathways:

$$\begin{aligned} M' &= a_M M - d_M M^2 - (k_1 T + k_2 S)\, M && (1)\\ B' &= \alpha_B B\,(B_T - B) + (k_4 S - k_3 M)\, B && (2)\\ S' &= a_S S - d_S S^2 + h_S B - (k_5 M + k_6 T)\, S && (3)\\ T' &= a_T T - d_T T^2 + k_7 B T && (4) \end{aligned}$$

The rates of various reactions that are involved in the interaction of the signaling pathways comprise most of the parameters of the model system and are represented by lower-case letters: a_X (activation rate of X), d_X (degradation rate of X), k_i (mass-action term involving two proteins or protein groups). Other parameters of the system are a_B, which is the activation rate of BMP; h_S, which is the activation rate of Smad1/4 due to BMP activity; and B_T, which corresponds to the maximum level of BMP activity in an embryonic cell.

This model also describes the case when there is no inhibition of the BMP-Smad1 pathway, i.e., when $M = 0$ and $T = 0$. In this case, equations 1-4 are reduced to the system:

$$\begin{aligned} B' &= \alpha_B B\,(B_T - B) + k_4 S B && (5)\\ S' &= a_S S - d_S S^2 + h_S B && (6) \end{aligned}$$

Steady state analysis of this system shows that one of the steady states (B^*, S^*) satisfies the equation

$$B^* = B_T + \left(\frac{k_4}{\alpha_B}\right) S^*, \tag{7}$$

which suggests that α_B should be negative to satisfy $B^* < B_T$. In this case, the rest of the parameters can assume nonnegative values. For the simulations in this paper, we chose parameter values that produce numerical solutions resembling observed biological results [21].

We aim to carry out computational simulations that are helpful in understanding the associated biological phenomenon. In particular, numerical bifurcation studies are performed to investigate relationships between key parameters identified by experimental biologists. Typically, biologists in cell signaling research are faced with the challenging task of understanding the interactions between many proteins in the signaling network. In a theoretical model that incorporates a network of proteins, mathematical theories and computational schemes on differential equations and dynamical systems aim to aid the biologist in elucidating the biochemical pathways.

3. **Computational Studies.**

The model is tested for qualitative results that are available in the literature. The findings of Uzgare, *et al.* [12] suggest that a 4 to 6-fold increase in MAPK activity is essential for the commitment of ectodermal cells to neural development. Equations 1-4 also reproduce this biological result, and the computational results are shown in this section.

To our knowledge, almost all of the parameter values needed for the computational simulations are unavailable in the literature. A long-term goal of our research is the determination of reasonable ranges for these parameter values, by using a validated mathematical model as a guide to solve the inverse problem of parameter estimation.

The *in vivo* observations of Uzgare, *et al.* [12] provide the basis for identifying the parameter values used in the simulations. The parameter values were selected to reproduce a qualitative result that mimics the temporal behavior of proteins being studied. Numerical solutions of the system were computed by integrating the model using `ode23s`, one of the differential equation solvers of MATLAB. Results arising from bifurcation analysis of this mathematical model are also given in this section. The numerical software AUTO [22] is used to investigate the bifurcations that are observed in the model.

3.1. **Temporal profiles.**

For the model to reproduce the effect of low MAPK activity, we chose parameter values that produce a numerical solution of a stable steady state with a low M value. This result is shown in Figure 2. For clarity, we only show two of the four variables. The time-dependent solution was obtained by numerical integration of the system given by equations 1-4. We note that this solution has a relatively high Smad1/4 activity level, which mimics the experimental result of significant Smad1/4 activity when MAPK levels are low.

This model is tested by increasing the activation rate of MAPK activity from $a_M = 1$ to $a_M = 5$, while keeping all other parameter values the same as in Figure 2. With this increase, the system exhibits a steady state solution with high MAPK activity but low Smad1/4 activity. This numerical result, which is shown in Figure 3, is consistent with the experimental finding that increased MAPK activity inhibits Smad1/4 activity and further commits ectodermal cells to neural development [10].

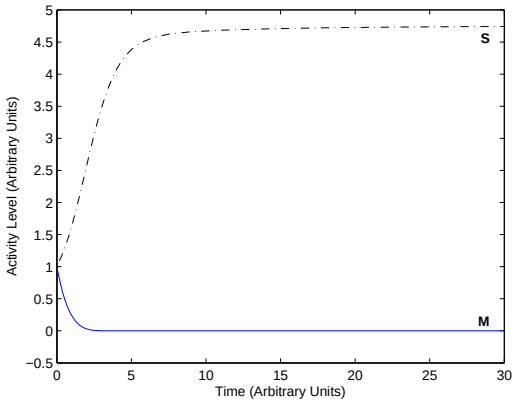

FIGURE 2. Activity levels of MAPK (solid line) and Smad1/4 complex (dashed) corresponding to low MAPK activity, which represent numerical solution of Equations 1-4 for the parameter values $a_M = 1.0, \alpha_B = -1.0, a_S = 1.0, a_T = 0.1, d_M = 0.2, d_S = 0.2, d_T = 0.2, h_S = 0.2, B_T = 10.0, k_1 = 1.0, k_2 = 1.0, k_3 = 1.0, k_4 = 1.0, k_5 = 0.3, k_6 = 0.1, k_7 = 1.0$, and the initial concentrations $M = 1.0, B = 1.0, S = 1.0, T = 1.0$. The activity levels vs. time in arbitrary time units.

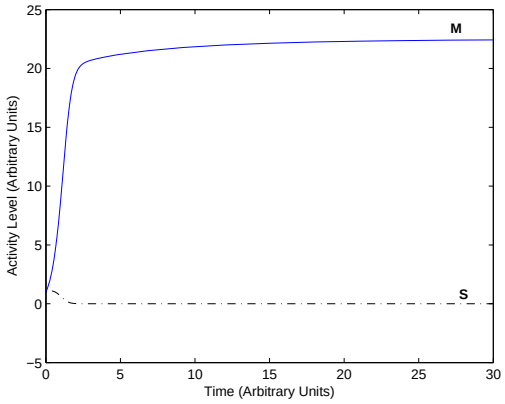

FIGURE 3. Activity levels of MAPK (solid line) and Smad1/4 complex (dashed) corresponding to high MAPK activity. Activation rate of MAPK activity a_M is increased from 1.0 to 5.0. All other parameter values are the same as in Figure 2.

3.2. **Bifurcation analysis.** To learn more about the steady states of the model system, a bifurcation diagram with respect to the parameter a_M is generated using AUTO. The diagram is shown in two different ways in Figures 4-5, one in terms of MAPK activity (M) and the other in terms of Smad1/4 activity (S). The diagram is generated with the steady state illustrated in Figure 2 as the starting point. This

steady state, where $a_M = 1$, MAPK activity is low and SMAD1/4 activity is high, is marked in the diagram with **x**. From this steady state, AUTO traces the entire diagram that reveals two meaningful transcritical bifurcations. The diagram also shows the steady state for $a_M = 5$ (marked with *) corresponding to Figure 3.

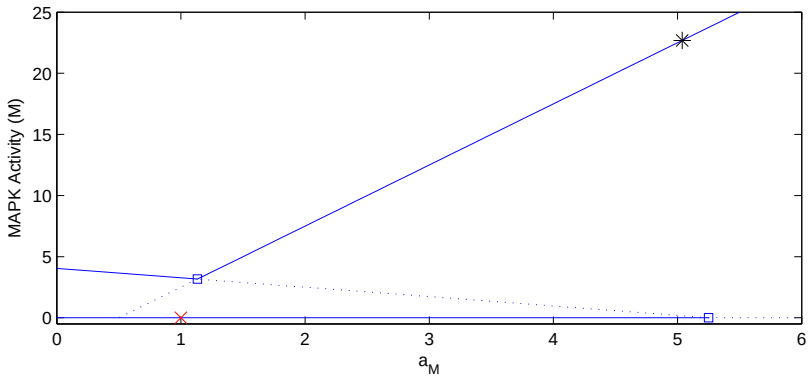

FIGURE 4. Bifurcation diagram with respect to a_M, in terms of MAPK activity

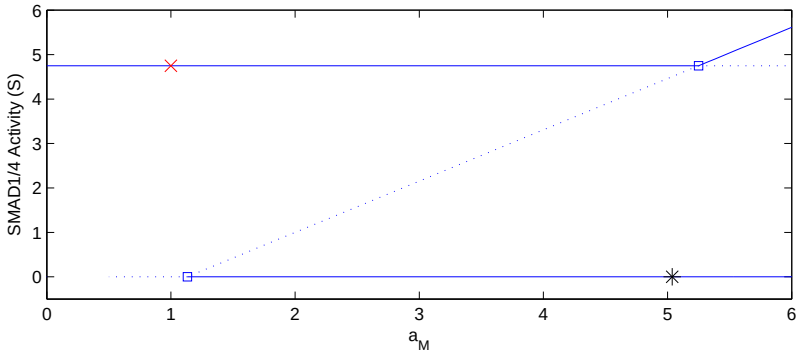

FIGURE 5. Bifurcation diagram with respect to a_M, in terms of Smad1/4 activity

The bifurcation diagram also reveals multiple steady states for certain values of the parameter a_M. For example, at $a_M = 5$, there is a second stable steady state which has no MAPK activity. Simulations using the MATLAB solver `ode23s` suggest that this steady state is achieved only when there is no initial MAPK activity, i.e., $M = 0$ at the start of the simulation (result not shown), and a slight MAPK activity at the start is enough for the system to achieve the steady state with a relatively high M value.

4. **Discussion.** The numerical simulations in Section 3 characterize the biological result that a 4 to 6-fold increase in MAPK activity inhibits Smad1/4 activity and triggers the neural fate of the embryo's ectodermal cells. Many other numerical

simulations can be performed to obtain various solutions, but bifurcation studies give a more comprehensive picture of the different kinds of steady states in the model. The bifurcation diagrams in Section 3 shows other steady states which may otherwise be overlooked. In particular, we have determined that there can be multiple steady states for the same set of parameter values and thus are also dependent on the initial values of the state variables.

We note that the parameter values used in the simulations of the model have been chosen to reproduce existing biological results. To our knowledge, almost all of these values are unavailable in the literature. As the model becomes further developed, it could be very useful for determining reasonable ranges for the rate constants of various biochemical reactions involved.

Mathematical analysis of the model system may also be beneficial in understanding the signaling pathways. In Section 1, the convenience of one of the parameters (α_B) assuming negative values is noted. In the case where B is the only nonzero state variable, the model system is reduced to the equation:

$$B' = \alpha_B B \left(B_T - B\right), \tag{8}$$

and a negative α_B implies that the steady state $B = 0$ is stable. This means that in order to maintain BMP activity in the BMP-Smad1 pathway, there has to be prior Smad1/4 activity.

As more biological information is known about the network of signaling pathways, the model system would have to be refined. The equations may need to be modified, but also, other equations representing rates of change of other proteins or protein groups may have to be added to the system. On the other hand, research on the signaling pathways can also benefit from further bifurcation studies with respect to other parameters that represent reaction rates deemed significant by the biologists. Two-parameter bifurcation studies are also helpful since they allow the investigation of the combined roles of two proteins in the biological network. These studies could suggest experimental designs that allow focus on two proteins at a time.

Acknowledgments. The authors would like to thank the referees for their valuable comments and suggestions. This work is supported in part by NSF grant DUE-0734294, which enabled undergraduate students (Tung Bui and Marsida Lisi) to participate in developing the mathematical model.

REFERENCES

[1] L. Niswander and G.R. Martin, *FGF-4 and BMP-2 have opposite effects on limb growth*, Nature, **361** (1993), 68–71.

[2] A. Neubüser, H. Peters, R. Balling and G.R. Martin, *Antagonistic interactions between FGF and BMP signaling pathways: a mechanism for positioning the sites of tooth formation*, Cell, **90** (1997), 247–255.

[3] B.P. Kruithof, B. van Wijk, S. Somi, M. Kruithof-de Julio, J.M. Pérez Pomares, F. Weesie, A. Wessels, A.F. Moorman and M.J. van den Hoff, *BMP and FGF regulate the differentiation of multipotential pericardial mesoderm into the myocardial or epicardial lineage*, Dev Biol., **295** (2006), 507–522.

[4] R.H. Xu, K.T. Ault, J. Kim, M.J. Park, Y.S. Hwang, Y. Peng, D. Sredni and H. Kung, *Opposite effects of FGF and BMP-4 on embryonic blood formation: roles of PV.1 and GATA-2*, Dev Biol., **208** (1999), 352–361.

[5] R.A. Buckland, J.M. Collinson, E. Graham, D.R. Davidson and R.E. Hill, *Antagonistic effects of FGF4 on BMP induction of apoptosis and chondrogenesis in the chick limb bud*, Mech Dev., **71** (1998), 143–150.

[6] E.M. De Robertis and H. Kuroda, *Dorsal-ventral patterning and neural induction in Xenopus embryos*, Ann. Rev Cell Dev Biol., **20** (2004), 285–308.
[7] C.D. Stern, *Neural induction: old problem, new findings, yet more questions*, Development, **132** (2005), 2007–2021.
[8] M. Kretzschmar, J. Doody and J. Massagué, *Opposing BMP and EGF signalling pathways converge on the TGF-β family mediator Smad1*, Nature, **389** (1997), 618–622.
[9] M. Goswami, A.R. Uzgare and A.K. Sater, *Regulation of MAP kinase by the BMP-4/TAK1 pathway in Xenopus ectoderm*, Dev Biol., **236** (2001), 259–270.
[10] A.K. Sater, H.M. El-Hodiri, M. Goswami, T.B. Alexander, O. Al-Sheikh, L.D. Etkin and J.A. Uzman, *Evidence for antagonism of BMP-4 signals by MAP kinase during Xenopus axis determination and neural specification*, Differentiation, **71** (2003), 434–444.
[11] E.M. Pera, A. Ikeda, E. Eivers and E.M. De Robertis, *Integration of IGF, FGF, and anti-BMP signals via Smad1 phosphorylation in neural induction*, Genes Dev., **17** (2003), 2993–2997.
[12] A.R. Uzgare, J.A. Uzman, H.M. El-Hodiri and A.K. Sater, *Mitogen-activated protein kinase and neural specification in Xenopus*, Proc. Natl. Acad. Sci. USA, **95** (1998), 14833–14838.
[13] C.F. Huang and J.E. Ferrell, *Ultrasensitivity in the mitogen-activated protein kinase cascade*, Proc. Natl. Acad. Sci. USA, **93** (1996), 10078-10083.
[14] L. Qiao, R.B. Nachbar, I.G. Kevrekidis and S.Y. Shvartsman, *Bistability and oscillations in the Huang-Ferrell model of MAPK signaling*, PLoS Comput Biol., **3** (2007), 1819–1826.
[15] M. Muller, M. Obeyesekere, G.B. Mills and P.T. Ram, *Network topology determines dynamics of the mammalian MAPK1,2 signaling network: bifan motif regulation of C-Raf and B-Raf isoforms by FGFR and MC1R*, FASEB J., **22** (2008), 1393-1403.
[16] J. Díaz, G. Baier, G. Martínez-Mekler and N. Pastor, *Interaction of the $IP_3 - Ca^{2+}$ and the FGF-MAPK signaling pathways in the Xenopus laevis embryo: a qualitative approach to the mesodermal induction problem*, Biophys. Chem., **97** 2002, 55-72.
[17] D.C. Clarke and X. Liu, *Decoding the quantitative nature of TGF-β/Smad signaling*, Trends in Cell Biology, **18** (2008), 430–442.
[18] B. Schmierer, A.L. Tournier, P.A. Bates and C.S. Hill, *Mathematical modeling identifies Smad nucleocytoplasmic shuttling as a dynamic signal-interpreting system*, Proc. Natl. Acad. Sci. USA, **05** (2008), 6608-6613.
[19] A. Hoffmann, O. Preobrazhenska, C. Wodarczyk, Y. Medler, A. Winkel, S. Shahab, D. Huylebroeck, G. Gross and K. Verschueren, *Transforming growth factor-beta-activated kinase-1 (TAK1), a MAP3K, interacts with Smad proteins and interferes with osteogenesis in murine mesenchymal progenitors*, J Biol Chem., **29**, (2005), 27271–27283.
[20] Liu and A.K. Sater, manuscript in preparation.
[21] H. Gohil, Chen, C.H. Lou and A.K. Sater, manuscript in preparation.
[22] E.J. Doedel, A.R. Champneys, T.F. Fairgrieve, Y.A. Kuznetsov, B. Sandstede and X. Wang, *AUTO 97: Continuation and Bifurcation Software for Ordinary Differential Equations (with HomCont)*, Technical Report, Concordia University, (1997).

Received August 2008; revised August 2009.

E-mail address: tecarroe@uhd.edu
E-mail address: tung_edu82@yahoo.com
E-mail address: marsil30@yahoo.com
E-mail address: asater@uh.edu
E-mail address: uzmana@uhd.edu